Hydrology and
Earth System
Sciences
Discussions

Open Access

Dominant climatic factor driving annual runoff change at catchments scale over China

Z. Huang[1,2,3] **and H. Yang**[1]

[1]State Key Laboratory of Hydro-Science and Engineering, Department of Hydraulic Engineering, Tsinghua University, Beijing, 100084, China
[2]Key Laboratory of Water Cycle and Related Land Surface Processes, Institute of Geographic Sciences and Natural Resources Research, Chinese Academy of Sciences, Beijing, 100101, China
[3]University of Chinese Academy of Sciences, Beijing, 100049, China

Discussion Paper | Discussion Paper | Discussion Paper | Discussion Paper |

HESSD

12, 12911–12945, 2015

Dominant climatic factor driving annual runoff change at catchments scale over China

Z. Huang and H. Yang

Title Page

Abstract | Introduction

Conclusions | References

Tables | Figures

◄◄ | ►►

◄ | ►

Back | Close

Full Screen / Esc

Printer-friendly Version

Interactive Discussion

Abstract

With global climate changes intensifying, the hydrological response to climate changes has attracted more attentions. It is beneficial not only for hydrology and ecology but also for water resources planning and management to reveal the impacts of climate change on runoff. It is of great significance of climate elasticity of runoff to estimate the impacts of climatic factors on runoff. In addition, there are large spatial variations in climate type and geography characteristics over China. To get a better understanding the spatial variation of runoff response to climate variables change and detect the dominant climatic factor driving annual runoff change, we chose the climate elasticity method proposed by Yang and Yang (2011), where the impact of the catchment characteristics on runoff was represented by a parameter n. The results show that the dominant climatic factor driving annual runoff is precipitation in the most part of China, net radiation in the lower reach of Yangtze River Basin, the Pearl River Basin, the Huai River Basin and the southeast area, and wind speed in part of the northeast China.

1 Introduction

Climate change has become increasingly significant, and it has important impacts on hydrology cycle and the water resource management. Changes in climatic factors and runoff have been observed in many different regions of China. The reduction of precipitation occurred in the Hai River Basin, the upper reach of the Yangtze River Basin and the Yellow River Basin, and the increase occurred in the in the western China (Yang et al., 2014). A 29 % decline of surface wind speed occurred in China during 1966 to 2011, which would have lead to a 1–6 % increase in runoff and a 1–3 % decrease in evapotranspiration at most regions in China (Liu et al., 2014). Most of the river basins in north China have exhibited obvious decline in mean annual runoff, such as the Shiyang River Basin (Ma et al., 2008), the Yellow River Basin (Yang et al., 2004; Tang et al., 2007; Cong et al., 2009), and the Hai River Basin (Ma et al., 2010). The

Z. Huang and H. Yang

Title Page

Abstract	Introduction
Conclusions	References
Tables	Figures

◄◄ ►►

◄ ►

Back Close

Full Screen / Esc

Printer-friendly Version

Interactive Discussion

Z. Huang and H. Yang

hydrologic processes have been influenced by different climatic factors. For example, decline in land surface wind speed could lead to decrease in evapotranspiration and changes in precipitation may affect water generation and concentration. However, the dominant climatic factor driving annual runoff change is still unknown in many catchments of China.

There are several approaches to investigate the feedback of annual runoff to climate change, such as the hydrologic models (Yang et al., 1998, 2000; Arnold et al., 1998; Arnold and Fohrer, 2005), the climate elasticity method (Schaake, 1990; Sankarasubramanian et al., 2001) and the statistics method (Vogel et al., 1999). Therein, the climate elasticity method was widely used in quantifying the effects of climatic factors on runoff, such as in the Yellow River Basin (Zheng et al., 2009; Yang and Yang, 2011), the Luan River Basin (Xu et al., 2013), the Chao–Bai Rivers Basin (Ma et al., 2010), and the Hai River Basin (Ma et al., 2008; Yang and Yang, 2011).

A simple climate elasticity method was firstly defined by Schaake (1990) to estimate the impacts of precipitation (P) on annual runoff (R):

$$\frac{\mathrm{d}R}{R} = \varepsilon_\mathrm{P}(P,R)\frac{\mathrm{d}P}{P}, \tag{1}$$

where ε_P is the precipitation elasticity. To consider the effects of precipitation and air temperature on runoff, Fu et al. (2007) calculated the runoff change as:

$$\frac{\mathrm{d}R}{R} = \varepsilon_a \frac{\mathrm{d}P}{P} + \varepsilon_b \frac{\mathrm{d}T}{T}, \tag{2}$$

where ε_a and ε_b are the precipitation elasticity and air temperature elasticity, respectively.

Five categories of methods can be used to estimate climate elasticity (Sankarasubramanian et al., 2001), and the analytical derivation method has been widely used in many studies because it is not only clear in theory but also does not need a large amount of historical observed data. Arora (2002) projected a equation to calcuated the response of runoff to precipitation and potential evaporation change:

$$\frac{\Delta R}{R} = \left[1 + \frac{\phi F_0'(\phi)}{1 - F_0(\phi)}\right]\frac{\Delta P}{P} - \frac{\phi F_0'(\phi)}{1 - F_0(\phi)}\frac{\Delta E}{E}, \tag{3}$$

where $\phi = E/P$ and $F_0(\phi)$ is a Budyko formula and $F_0'(\phi)$ is the derivation to ϕ. The climate elasticity of runoff was evaluated in the upper reach of the Yellow River Basin by using Eq. (3) (Zheng et al., 2009). To evaluate the impact from other climatic factors, Yang and Yang (2011) proposed an analytical method, which was based on the Penman equation and the annual water balance equation, to quality the runoff change to changes in different climatic factors. By taking advantage of the mean annual climatic factors in the study period, the runoff elasticity to precipitation (P), mean air temperature (T), net radiation (R_n), relative humidity (RH), and wind speed (U_2) were derived, and the runoff change can be expressed as follows:

$$\frac{dR}{R} = \varepsilon_P \frac{dP}{P} + \varepsilon_{Rn}\frac{dR_n}{R_n} + \varepsilon_T dT + \varepsilon_{U_2}\frac{dU_2}{U_2} + \varepsilon_{RH}\frac{dRH}{RH}, \tag{4}$$

where ε_P, ε_{R_n}, ε_T, ε_{U_2}, and ε_{RH} are the runoff elasticity to precipitation (P), net radiation (R_n), mean air temperature (T), wind speed (U), and relative humidity (RH), respectively. However, this method was only tested in several catchments of the non-humid Northern China.

There are large spatial variations in both geography characteristics and climate type over China, which would result in a large variation in the hydrologic response to climate change. Therefore, the current study aims to: (1) further validating the method proposed by Yang and Yang (2011), (2) evaluating the climate elasticity of climatic factors to runoff at catchments scale over China, and (3) estimating the impact of climate variation on runoff and then detecting the dominant climatic factor driving annual runoff change.

2 Climate elasticity method based on the Budyko hypothesis

At catchment scale, there is abvious relationship between evaporation, precipitation and potential evaporation, which is referred as the Budyko hypothesis (Budyko, 1961). An analytical equation of the Budyko hypothesis was inferred by Yang et al. (2008):

$$E = \frac{E_0 P}{\left(P^n + E_0^n\right)^{1/n}}, \tag{5}$$

where the parameter n represents the characteristics of the catchment, for example land use and coverage change, vegetation, slope and climate seasonality (Yang et al., 2014). The water balance equation can be simplified as $P = E + R$ at catchment scale for the long term, so runoff can be expressed as follows:

$$R = P - \frac{E_0 P}{\left(E_0^n + P^n\right)^{1/n}}. \tag{6}$$

To attribute the contribution of changes in P and E_0 to runoff, Yang and Yang (2011) derived a new equation:

$$\frac{dR}{R} = \varepsilon_1 \frac{dP}{P} + \varepsilon_2 \frac{dE_0}{E_0}, \tag{7}$$

where ε_1 and ε_2 are the climate elasticity of runoff to P and E_0, respectively; and they can be estimated as $\varepsilon_1 = \frac{(1 - \partial E/\partial P)P}{P - E}$ and $\varepsilon_2 = -\frac{\partial E/\partial E_0 E_0}{P - E}$. The potential evaporation E_0 (mm day^{-1}) can be evaluatedby the Penman equation (Penman, 1948):

$$E_0 = \frac{\Delta}{\Delta + \gamma}(R_n - G)/\lambda + \frac{\gamma}{\Delta + \gamma} 6.43(1 + 0.536 U_2)(1 - \mathrm{RH})e_s/\lambda, \tag{8}$$

and the physical meaning of these symbols were shown in Table 1.

Similar to Eq. (7), the response of potential evaporation to climatic factors can be estimated as:

$$\frac{\mathrm{d}E_0}{E_0} = \varepsilon_3 \frac{\mathrm{d}R_n}{R_n} + \varepsilon_4 \mathrm{d}T + \varepsilon_5 \frac{\mathrm{d}U_2}{U_2} + \varepsilon_6 \frac{\mathrm{d}RH}{RH}, \tag{9}$$

where $\varepsilon_3, \varepsilon_4, \varepsilon_5, \varepsilon_6$ are the elasticity of potential evaporation to net radiation, air temperature, wind speed and relative humidity, respectively. Therein, $\varepsilon_3 = \frac{R_n}{E_0} \frac{\partial E_0}{\partial R_n}$, $\varepsilon_4 = \frac{1}{E_0} \frac{\partial E_0}{\partial T}$, $\varepsilon_5 = \frac{U_2}{E_0} \frac{\partial E_0}{\partial U_2}$, and $\varepsilon_6 = \frac{RH}{E_0} \frac{\partial E_0}{\partial RH}$. Due to the complex relationship between E_0 and T, the value of $\frac{\partial E_0}{\partial T}$ was calculated by finite difference method, while $\frac{\partial E}{\partial P}$, $\frac{\partial E}{\partial E_0}$, $\frac{\partial E_0}{\partial R_n}$, $\frac{\partial E_0}{\partial U_2}$ and $\frac{\partial E_0}{\partial RH}$ were calculated by finite differential method.

Substitution of Eq. (9) into Eq. (7) leads to:

$$\frac{\mathrm{d}R}{R} = \varepsilon_1 \frac{\mathrm{d}P}{P} + \varepsilon_2 \varepsilon_3 \frac{\mathrm{d}R_n}{R_n} + \varepsilon_2 \varepsilon_4 \mathrm{d}T + \varepsilon_2 \varepsilon_5 \frac{\mathrm{d}U_2}{U_2} + \varepsilon_2 \varepsilon_6 \frac{\mathrm{d}RH}{RH}. \tag{10}$$

Denoted Eq. (10) as follows:

$$R^* = P^* + R_n^* + T^* + U_2^* + RH^*, \tag{11}$$

where P^*, R_n^*, T^*, U_2^* and RH^* symbolize the runoff changes caused by the changing in P, R_n, T, U_2 and RH, respectively. The largest one among them is considered as the dominant climatic factor driving annual runoff change.

3 Data and method

3.1 Study region and data

Catchment information data set was collected from the Ministry of Water Resources of the People's Republic of China (Water Resources and Hydropower Planning and

Design General Institute, 2011). In the data set, catchment boundary and runoff ratio were available. Chinese water resources zoning was divided level by level, and there are 10 first-level basins, 80 s-level river basins and 210 third-level river basins (shown in Fig. 1a). Therein, there are no observed meteorological data in Taiwan Island and no runoff in two inland catchments in Xinjiang province. Hence 207 third-level catchments were selected in this study.

Meteorological data, obtained from 736 weather stations during the period 1961–2010 from the China Meteorological Administration (CMA), included precipitation, surface mean air temperature, maximum air temperature, minimum air temperature, relative humidity, sunshine hours, and wind speed. In addition, daily solar radiation during the period 1961–2010 was collected from 118 weather stations.

To get the annual climatic factors in each catchment, firstly, a 10 km grid data set, which covers the study area, was prepared for interpolation from the observed meteorological data. Secondly, according to the 10 km grid data set, the average values of cliamte factors of each catchment were calculated. The interpolation method for climatic factors were an inverse-distance weighted technique, except air temperature which must consider the influence of elevation (Yang et al., 2006).

Since only 118 weather stations directly measured solar radiation, the daily net radiation R_n (MJ m^{-2} day^{-1}) was calculated as:

$$R_n = (1 - \alpha_s)R_s - \sigma \left[\frac{(T_{max} + 273.15)^4 + (T_{min} + 273.15)^4}{2} \right] \left(0.1 + 0.9\frac{n}{N} \right)$$

$$\times \left(0.34 - 0.14\sqrt{\frac{RH}{100}e_s} \right), \tag{12}$$

and the physical meaning of these symbols were shown in Table 2. R_s was calculated by using the Angström formula (Angström, 1924):

$$R_s = \left(a_s + b_s \times \frac{n}{N} \right) R_a, \tag{13}$$

where R_a is the extra-terrestrial radiation; and a_s and b_s are parameters which were calibrated using the data at the 118 stations with solar radiation observations (Yang et al., 2006). In Eq. (12), e_s is estimated as:

$$e_s = 0.3054 \left[\exp\left(\frac{17.27 T_{max}}{T_{max} + 237.3} \right) + \exp\left(\frac{17.27 T_{min}}{T_{min} + 237.3} \right) \right]. \tag{14}$$

Wind speed at a height of 2 m (U_2, m s^{-1}) can be calculated by the observed wind speed at 10 m height (Allen et al., 1998):

$$U_2 = U_z \frac{4.87}{\ln(67.8z - 5.42)} = 0.75 U_{10}. \tag{15}$$

Based on Eq. (6), the runoff ratio (α) can be estimated as follows:

$$\alpha = \frac{R}{P} = 1 - \frac{E_0}{\left(E_0^n + P^n \right)^{1/n}}. \tag{16}$$

Furthermore, the catchment characteristics parameter n was calculated according to α, E_0 and P.

3.2 Validation of the climate elasticity method

Two steps were taken for the validation of the climate elasticity method, namely validating Eq. (7) and validating Eq. (9).

To validate Eq. (7), two catchments were chosen, namely the Luan River Basin and the upper Hanjiang River Basin (shown in Fig. 1b). The Luan River Basin, located in north China, is a part of Hai River Basin. It has a mean annual precipitation of 455 mm, 75–85 % of which concentrates from June to September. The Hanjiang River Basin, lying in the middle and lower reaches of the Yangtze River Basin, which is the largest tributary of the Yangtze River, finally flows into Danjiangkou reservoir and has a length

Z. Huang and H. Yang

of about 925 km and an elevation of 3500–88 m. In the two catchments, runoff has a remarkable change, and the causes for runoff change were analyzed by hydrological models. Xu et al. (2013) assessed the response of annual runoff to anthropogenic activities and climate change in the Luan River Basin by using the GBHM model. Sun et al. (2014) explored the contributions from climate change and catchment properties variation to runoff change in Danjiangkou Basin by using three different methods including climate elasticity and decomposition methods, and the dynamic hydrological modeling method. To validate the climate elasticity method, the results given by Eq. (7) were compared with the results in references Xu et al. (2013) and Sun et al. (2014).

Equation (9) is the first-order Taylor expansion of Penman equation. On one hand, we firstly evaluated the climate elasticity of potential evaporation to air temperature, net radiation, relative humidity, wind speed and the change in these climatic factors, and further estimated the change in potential evaporation according Eq. (9), denoted as E_0^*. On the other hand, we calculated the potential evaporation change (E_0^{**}) as:

$$\frac{dE_0}{E_0} = \frac{f(T + dT, R_n + dR_n, U_2 + dU_2, RH + dRH) - f(T, R_n, U_2, RH)}{E_0}, \tag{17}$$

where the function f represents the Penman equation. Then, the first approximation E_0^* was compared with E_0^{**}, to evaluation the error of Eq. (9).

3.3 Trend analysis

The Mann–Kendall (MK) nonparametric test (Kendall, 1990) is an effective statistical tool for trend detection, especially for hydrological and meteorological time series (Mainment, 1993). The MK nonparametric test is widely used for its convenient calculation processes. The sample data are not necessary to obey some specific distribution, but they must be serially indenpendent. In this study, we firstly evaluated the significance levels of the trend of the hydrological and meteorological time series which were set at 0.05 and 0.1, and then estimated the slope of the trend:

$$\beta = \text{median} \left[\frac{(x_j - x_i)}{(j - i)} \right], \tag{18}$$

for all $i < j$; where β is the magnitude of trend, and $\beta > 0$ indicates an increasing trend, and $\beta < 0$ indicates a decreasing trend.

4 Result

4.1 Validation of the climate elasticity method

Table 3 showed the comparison of climate contribution to runoff which were estimated by the climate elasticity method and the hydrological models. The climate contribution to runoff is −14 and −21.4 % in the upper Luan River Basin, 12.4 and 9.1 % in the lower Luan River Basin and −19.6 and −19.0 % in the upper Hanjiang River Basin, which were estimated by the climate elasticity method and the hydrological models respectively. The result provided a strong evidence for using the climate elasticity method to evaluate the climate elasticity and the response of runoff to climate change both in humid and arid catchments.

Figure 2a showed the relationship between the potential evaporation change evaluated by Eq. (9) and that evaluated by Eq. (17), and most of the point were around the line $y = x$. The relative errors (shown in Fig. 2b) mostly ranged from −3–1 %. High correlativity of them and the small relative errors showed the accuracy of Eq. (9), which maked it possible to express potential evaporation change as a function of cliamtic factors variation.

4.2 The mean annual climatic factors

The mean annual precipitation, net radiation, air temperature, wind speed, and relative humidity for each catchment during 1961–2010 were shown in Fig. 3. The mean annual

precipitation in China, ranged from $30 \, \mathrm{mm \, a^{-1}}$ in the northwest inland to $1883 \, \mathrm{mm \, a^{-1}}$ in the southeast coastal area, and it had a typical spatial variation of decreasing from the southeast to the northwest.

The net radiation differed from 3–10 ($\mathrm{MJ \, m^{-2} \, day^{-1}}$) in China, of which the largest value occurred in the Qinghai–Tibet Plateau and the lowest value occurred in Sichuan Basin. The mean annual air temperature in China had a range of -3.3–$23.8\,^{\circ}\mathrm{C}$, with a typical spatial variation of decreasing from the south to the north. The wind speed in $2 \, \mathrm{m}$ height in China ranged from 1 to $4 \, \mathrm{m \, s^{-1}}$, and the high value occurred in the north and the coastland and the lowest value occurred in Sichuan Basin. The relative humidity, which ranged from $35\,\%$ in the northwest to $82\,\%$ in the southeast, had a positive correlation with precipitation. According to Eq. (6), we can evaluate the mean annual runoff. The annual mean runoff had a range of 0 to $1176 \, \mathrm{mm \, a^{-1}}$ which had a similar spatial variation with that of pricipitation.

4.3 Climate elasticity of the 207 catchments

Figure 4 showed the climate elasticity of runoff to the climatic factors for each catchment. In the 207 catchments, precipitation elasticity ε_P ranged from 1.1 to 4.75 (2.0 on average), indicating that $1\,\%$ change in precipitation leads to 1.1–$4.75\,\%$ change in runoff. The lowest value of ε_P, ranged from 1.1 to 1.5, occurred in southern China. The highest value of ε_P mostly occurred in the Huai River Basin, the Liao River Basin, and the Hai River Basin, and the lower reach of Yellow River Basin.

A $1\,\%$ R_n change caused -0.1 to $-2\,\%$ (-0.5 on average) runoff change. The high value of $-0.5 < \varepsilon_{R_n} < -2.0$ mostly occurred in the Huai River Basin, the Liao River Basin, and the Hai River Basin, and the downstream of Yellow River Basin, and the relatively small value of $-0.1 < \varepsilon_{R_n} < -0.5$ mostly occurred in southern and northwest China. The air temperature elasticity, ranging from -0.1 to 0.1, indicted that a 1 centigrade degree increase in air temperature will result in -10–$10\,\%$ increase in runoff. The sensibility of runoff to the air temperature change varied from geographic position

and had no rules, and the reason will be discussed in discussion part. The value of ε_{U_2} ranged from -0.01 to -0.94 (-0.22 on average). The high value of $-0.95 < \varepsilon_{U_2} < -0.5$ mostly occurred in the north China. The value of ε_{RH} ranged from 0.05 to 3 (0.74 on average), and the distributions of them agreed with that of precipitation.

4.4 Changes in the climatic factors

The changes in climatic factors were shown in Fig. 5. There is a large spatial variation in precipitation change which increased in the northwest China (ranging from 5 to 11 % decade^{-1}, $p < 0.05$) and decreased in Yellow River Basin, Hai River Basin and the upper reach of Yangtze River Basin (ranging from -5 to -2.5 % decade^{-1}, $p < 0.05$), but there were no significant change trend shown in 63 % of these 207 catchments.

Net radiation showed a decrease in most catchments. Large decrease (ranging from -6 to -3 % decade^{-1}) occurred in the Hai River Basin, the Huai River Basin and the lower reach of Yangtze River Basin ($p < 0.05$), while small decrease (ranging from -3 to -0 % decade^{-1}) occurred in the majority of the northern China. No significant change trend was shown in the Qinghai–Tibet Plateau.

Air temperature increased all over the China. Large increase (ranging from 0.4 to 0.8 °C decade^{-1}) mainly occurred in the northern China ($p < 0.05$), while small decrease (ranging from 0 to 0.4 °C decade^{-1}) occurred in the majority of the southeast.

Wind speed decreased in most catchments, ranging from -11 % decade^{-1} in the southeast to -1 % decade^{-1} in the upper reach of Yangtze River Basin. Only 5 catchment showed significant ($p < 0.05$) increase in wind. Relative humidity increased in the western China (the maximum is about 3 % decade^{-1}) and decreased in the southeast China and the Yangtze River Basin (ranging from -1.7 to -0.5 % decade^{-1}). The change trend of relative humidity agreed with the change of precipitation.

Full Screen / Esc

Printer-friendly Version

Interactive Discussion

4.5 Contributions of climatic factors to the runoff change

Figure 6 showed the contributions of climatic factors to the runoff change. The contribution of precipitation to the change of runoff had a distinctspatial variation. Positive contribution occurred in the western China and the southeast of China, especially in the northwest where the contribution of precipitation to runoff change ranges from 12 to 25 % decade^{-1}. While negative contribution mainly occurred in the central and northeast China.In the middle reach of the Yellow River Basin and the Hai River Basin, the negative contribution reaches the most, ranging from −18 to −10 % decade^{-1}.

Positive contribution of net radiation to runoff change occurred in most catchments except for the Qinghai–Tibet Plateau. In the Hai River Basin, the positive contribution reached the most, ranging from 3 to 9 % decade^{-1}, while in other catchments the net radiation effected the runoff small.

Positive contribution of air temperature to runoff change occurred in the Qinghai–Tibet Plateau and the northern part of the northeast China, while negative contribution mainly occurred in northwest and the eastern China except for the northeast China. Positive contribution and negative contribution of air temperature to runoff change were both small when compared with other climatic factors.

Positive contribution of wind speed to runoff change occurred in most catchments except for part of the upper reach of Yangtze River Basin. In the Hai River Basin and the Liao River Basin, the positive contribution reached the most, ranging from 2 to 6 % decade^{-1}, while in other catchments the wind speed effected the runoff small.

Negative contribution of relative humidity to runoff change occurred in most catchments except for part of the northwest where the positive contribution of relative humidity to the change of runoff ranges 0–2 % decade^{-1}.

Figure 7 showed the contribution of climate factors to runoff change, which was defined as the sum of the contribution of climatic factors. Generally speaking, climate change had a negative contribution on runoff in Hai River Basin, part of the Liao River Basin, the middle and lower reaches of Yellow River Basin and the southeast China,

and had a positive contribution in the northwest, part of the northeast and the southeast China. Therein, the largest positive contribution from climate change to runoff occurred in the northwest, ranging from 10 to 30 % decade^{-1}, while the largest negative contribution occurs in the middle reach of the Yellow River Basin and the Hai River Basin, ranging from −13 to −8 % decade^{-1}.

4.6 The dominant climatic factors driving runoff change

Figure 8 showed the dominant climatic factors driving runoff in the 207 catchments. In most catchments, the runoff change was dominated by precipitation. In addition, the runoff change was mainly determined by net radiation in the lower reach of the Yangtze River Basin, the Pearl River Basin, the Huai River Basin and the southeast area, and by wind speed in part of the northeast, part of the Inner Mongolia and part of the northeast Area.

5 Discussion

5.1 Climate elasticity

The climate elasticity method is widely used to evaluate hydrologic cycle in many catchments in China. Yang et al. (2014) calibrated precipitation elasticity to be 1.1 to 4.8 in China, which is the same with our result. What's more, in previous study, the precipitation elasticity were evaluated as 2.6 in the Luan River Basin (Xu et al., 2013), as 2.4 in the Chao–Bai Rivers Basin (Ma et al., 2010), as 1.4 to 1.7 in the Poyang Lake (Sun et al., 2013), as 1.4 for the Beijiang River catchment of the Pearl River Basin (Wang et al., 2013), as 1.0–2.0 in the Dongjiang River catchment of the Pearl River Basin (Jiang et al., 2007). Those results were also in good agreement with our results for ε_P in the same regions.

Wind speed elasticity, which stands for the sensitivity of annual runoff change to wind speed change, was negative across China with small sensitivity in the southern

China and high sensitivity in the Northern China. Yang and Yang (2011) calculated wind speed elasticity $\varepsilon_U = -0.3$ for the Futuo River catchment of the Hai River Basin by using the climate elasticity method, which was same with our result for the same catchment. Tang et al. (2013) estimated $\varepsilon_U = -0.59$ for the entire Yellow River Basin; Yang and Yang (2011) estimated ε_U ranging of -0.8 to -0.1 in the 89 catchments of the Hai River and the Yellow River Basins of China. Those results were similar to our result in the same regions.

The net radiation elasticity and the relative humidity elasticity agreed with the result evaluated by Yang and Yang (2011) in Futuo River catchment of the Hai River Basin and 89 catchments of the Hai River and the Yellow River Basins of China and are also similar to the result calculated by Tang et al. (2013) in the Yellow River Basin.

The air temperature elasticity ranges from -0.1 to 0.1, which were similar to other studies in the same regions (Yang and Yang, 2011; Tang et al., 2013; Yang et al., 2014). However, the air temperature elasticity is obvious small when compared to other climatic elasticities. Next, we will discuss the cause why air temperature elasticity is small. Air temperature elasticity is calculated by the following equation:

$$\varepsilon_T = \varepsilon_2 \varepsilon_4 = \varepsilon_2 \frac{1}{E_0} \frac{\partial E_0}{\partial T}\Big|_{X=\overline{X}}, \tag{19}$$

where ε_2 is the runoff elasticity to potential evaporation, ranging from -3 to 0 in China. So the value of ε_T is mainly determined by $\frac{\partial E_0}{\partial T}$. Figure 9 showed the relationship between T and $\frac{\partial E_0}{\partial T}$ in 207 basins of China. $\frac{\partial E_0}{\partial T}$ varied in different basins, but it had increase trend as T increasing. What's more, when $T < 10\,°C$, $\frac{\partial E_0}{\partial T}$ was negative mostly, while when $T > 10\,°C$, $\frac{\partial E_0}{\partial T}$ was positive mostly. Next, we will analyze the value of $\frac{\partial E_0}{\partial T}$ by the differential method. Denoting Eq. (8) as $E_0 = f_1(\Delta, e_s)$, and we can express (kPa$°C^{-1}$) and e_s (kPa) as $\Delta = f_2(T)$ and $e_s = f_3(T)$, respectively. Due to their substitution, $\frac{\partial E_0}{\partial T}$ can be expressed as:

$$\frac{\partial E_0}{\partial T} = \frac{\partial E_0}{\partial \Delta}\frac{\partial \Delta}{\partial T} + \frac{\partial E_0}{\partial e_s}\frac{\partial e_s}{\partial T}, \tag{20}$$

where $\frac{\partial E_0}{\partial \Delta} = \frac{\gamma}{(\Delta+\gamma)^2}\left[\frac{(R_n-G)-6.43(1+0.536U_2)(1-\mathrm{RH})e_s}{\lambda}\right]$ and $\frac{\partial E_0}{\partial e_s} = \frac{\gamma}{\Delta+\gamma}6.43(1+0.536U_2)(1-$ RH$)/\lambda$. Figure 10 showed the trend of and e_s as the change of temperature according to the connection between Δ and T and between e_s and T. $\frac{\partial E_0}{\partial \Delta}$ ranged from −5.5 to 9.3 (0.22 on average), while $\frac{\partial E_0}{\partial e_s}$ ranged from 0.3 to 1.9 (0.85 on average). From the results, it could be found that the absolute value of $\frac{\partial E_0}{\partial \Delta}$ and $\frac{\partial E_0}{\partial e_s}$ is small and the sign of $\frac{\partial E_0}{\partial T}$ depends on $\frac{\partial E_0}{\partial \Delta}$. Furthermore, the derivatives and e_s with respect to temperature is small, which leads to the small value of $\frac{\partial E_0}{\partial T}$.

Changing in air temperature would affect the atmosphere, which results in potential evaporation change, further affecting runoff. What's more changeing air temperature would also affect atmospheric movement, resulting in precipitation change (Gardner, 2009). In fact, changes in air temperature have great effects on runoff. The climate elasticity method only analyzes the direct impact of air temperature on runoff but ignores the indirect impact. Chiew et al. (2009) evaluated that the indirect impact of air temperature on runoff would be important, and a degree global warming will result in −10–3 % changes in runoff.

5.2 Effect of climate change to runoff

Recently, many studies have been carried out to assess the effects of climate change on runoff. Xu et al. (2013) reported that the runoff increase caused by cliamte change were 8.8 and 9.2 mm simulated by GBHM and the climate elasticity model in Luan River Basin. Tang et al. (2013) analyzed response of natural runoff to climate change in the Yellow River Basin by using the climate elasticity method and SWAT model, and the two methods also gave similar conclusion. Their results agreed with that revealed in this study.

Previous studies reported that precipitation decrease was the dominant factor of declining runoff in Futuo River catchment (Yang and Yang, 2011) and the Yellow River Basin (Tang et al., 2013), which agreed with our result.

Remarkably, in some catchments of the northeast, the Inner Mongolia and the northwest Area, declining wind speed has the greatest contribution to runoff change. McVicar et al. (2012) stressed that the impact of wind speed change on actual evapotranspiration and runoff was situation dependent. Wind speed decline tended to result in the decline of actual evapotranspiration and complementary increase of streamflow in wet river basins but has little impacts in dry basins (Liu et al., 2014), which was similar to our results. In previous studies, when assessing the impacts of changes in meteorological factors on runoff in China, wind speed declines were often identified as being important (Tang et al., 2011; Liu et al., 2014). And in the part of the northeast, part of the Inner Mongolia and part of the northwest area, due to the small hydrology changes and the stable precipitation, wind speed decline became the main contribution factor to runoff change.

The dominant climatic factor to runoff change was determined by the geographic conditions and climate. In this study, we analyzed the contribution of climatic factors to runoff change by the climate elasticity method which only stresses on the direct impact of climate change on runoff but ignores the relation between climatic factors. And the relationship needs further study.

5.3 Error analysis

In Eq. (10), the net radiation R_n and the air temperature T were considered as two independent elements. But in fact, according to Eqs. (12) and (13) the net radiation R_n is associated to the air temperature T. To verify the impact of the relationship between net radiation and air temperature on Eq. (12), the effect of change in air temperature to change in net radiation R_n must be evaluated as follows:

$$dR_n = \frac{\Delta R_n}{\Delta T} dT. \qquad (21)$$

If the effect of T on R_n was ignored, the relative error was less than 1 %, which was evaluated by Yang and Yang (2011) in the Futuo River Basin.

In addition, Eq. (10) is a first-order approximation, which probably results in errors in the estimating of climate elasticity. Yang et al. (2014) evaluated that when the changes in potential evapotranspiration (ΔE_0) and precipitation (ΔP) are not large, the error of ε_P caused by first-order approximation can be discounted, but the error will increase with changes increasing with a 0.5–5 % relative error in ε_P. When $\Delta P = 10$ mm and a 5–50 % relative error in ε_P When $\Delta P = 100$ mm. Bao et al. (2012) estimated that a 100 mm increase in precipitation causes 20 % increase in ε_P by adopting the Variable Infiltration Capacity (VIC) model.

6 Conclusions

In this study, we used the climate elasticity method to reveal the dominant climatic factor driving annual runoff change over China. We first validated the climate elasticity method which was firstly derived by Yang and Yang (2011). On account of China being a vast country with remarkable spatial differences in climate and geography characteristics, we divided China into 207 catchments, and then evaluated the climate elasticity of runoff to precipitation, net radiation, air temperature, wind speed and relative humidity, and estimated the contribution of climate factors to runoff change for each catchment.

In the 207 catchments, precipitation elasticity, which was low in in southern China or small part of the northwest and high in the Liao River Basin, the Hai River Basin, the Huai River Basin, ranged from 1.1 to 4.75 (2.0 on average). The air temperature elasticity, ranging from −0.1 to 0.1. Net radiation elasticity which ranges from −0.1 to −2 (−0.5 on average), wind speed elasticity which ranged from −0.01 to 0.94 (−0.22 on

average) and relative humidity elasticity which ranged from 0.05 to 3 (0.74 on average) had similar distributions with precipitation elasticity.

There was a large spatial variation in climatic factors change. Precipitation increased in the northwest China and decreased in Yellow River Basin, Hai River Basin and the upper reach of Yangtze River Basin. Net radiation showed a decrease in most catchments. Air temperature increased all over the China. Wind speed decreased in most catchments and the change of relative humidity agrees with the change of precipitation.

Climate change had a negative contribution on runoff in part of the Liao River Basin, the Hai River Basin, the middle and lower reaches of Yellow River Basin and the southeast China, and had a positive contribution in the northwest, part of the northeast and the southeast China. what's more, the largest positive contribution from climate change to runoff ranged from 10 to 30 % decade^{-1} in the northwest China, while the largest negative contribution ranged from -13 to -8 % decade^{-1} in the middle reach of the Yellow River Basin and the Hai River Basin.

Regarding the dominant climatic variable driving runoff change, it was precipitation in most of the 207 catchments, net radiation in the lower reach of Yangtze River Basin and the southeast, and wind speed in part of the northeast.

References

Allen, R., Pereira, L., Raes, D., and Smith, M.: Crop evapotranspiration: guidelines for computing crop water requirements, FAO Irrigation Drainage Paper 56, FAO, Rome, 1998.

Angström, A.: Solar and terrestrial radiation, Q. J. Roy. Meteorol. Soc., 50, 121–126, 1924.

Arnold, J. G. and Fohrer, N.: SWAT2000: current capabilities and research opportunities in applied watershed modelling, Hydrol. Process., 19, 563–572, 2005.

Arnold, J. G., Srinivasan, R., Muttiah, R. R., and Williams, J. R.: Large hydrologic modeling and assessment Part 1: Model development, J. Am. Water Resour. As., 34, 73–89, 1998.

Arora, V. K.: The use of the aridity index to assess climate change effect on annual runoff, J. Hydrol., 265, 164–177, 2002.

5 Bao, Z., Zhang, J., Liu, J., Wang, G., Yan, X., Wang, X., and Zhang, L.: Sensitivity of hydrological variables to climate change in the Haihe River Basin, China, Hydrol. Process., 26, 2294–2306, 2012.

Budyko, M. I.: The heat balance of the Earth's surface, Sov. Geogr., 2, 3–13, 1961.

Chiew, F., Teng, J., Vaze, J., and Kirono, D.: Influence of global climate model selection on
10 runoff impact assessment, J. Hydrol., 379, 172–180, 2009.

Cong, Z., Yang, D., Gao, B., Yang, H., and Hu, H.: Hydrological trend analysis in the Yellow River Basin using a distributed hydrological model, Water Resour. Res., 45, 335–345, 2009.

Fu, G., Charles, S. P., and Chiew, F. H. S.: A two-parameter climate elasticity of streamflow index to assess climate change effects on annual streamflow, Water Resour. Res., 43, W11419,
15 doi:10.1029/2007WR005890, 2007.

Gardner, L. R.: Assessing the effect of climate change on mean annual runoff, J. Hydrol., 379, 351–359, 2009.

Jiang, T., Chen, Y. D., Xu, C. Y., Chen, X., Chen, X., and Singh, V. P.: Comparison of hydrological impacts of climate change simulated by six hydrological models in the Dongjiang Basin, south
20 China, J. Hydrol., 336, 316–333, 2007.

Kendall, M. G. and Gibbons, J. D.: Rank Correlation Methods, Oxford University Press, Oxford, 1990.

Liu, X., Zhang, X.-J., Tang, Q., and Zhang, X.-Z.: Effects of surface wind speed decline on modeled hydrological conditions in China, Hydrol. Earth Syst. Sci., 18, 2803–2813,
25 doi:10.5194/hess-18-2803-2014, 2014.

Ma, H., Yang, D., Tan, S. K., Gao, B., and Hu, Q.: Impact of climate variability and human activity on streamflow decrease in the Miyun Reservoir catchment, J. Hydrol., 389, 317–324, 2010.

Ma, Z., Kang, S., Zhang, L., Tong, L., and Su, X.: Analysis of impacts of climate variability and human activity on streamflow for a river basin in arid region of northwest China, J. Hydrol.,
30 352, 239–249, 2008.

Mainment, D. R.: Handbook of Hydrology, McGraw-Hill, New York, 1993.

Title Page

Abstract | Introduction

Conclusions | References

Tables | Figures

◀ | ▶▶

◀ | ▶

Back | Close

Full Screen / Esc

Printer-friendly Version

Interactive Discussion

Discussion Paper | Discussion Paper | Discussion Paper | Discussion Paper

Mcvicar, T. R., Roderick, M. L., Donohue, R. J., and Van Niel, T. G.: Less bluster ahead? Ecohydrological implications of global trends of terrestrial near-surface wind speeds, Ecohydrology, 5, 381–388, 2012.

Penman, H. L.: Natural evaporation from open water, bare soil and grass, P. Roy. Soc. Lond., 193, 120–145, 1948.

Sankarasubramanian, A., Vogel, R. M., and Limbrunner, J. F.: Climate elasticity of streamflow in the United States, Water Resour. Res., 37, 1771–1781, 2001.

Schaake, J. C.: From climate to flow, in: Climate Change and US water resources, edited by: Waggoner, P. E., John Wiley, New York, 177–206, 1990.

Sun, S., Chen, H., Ju, W., Song, J., Zhang, H., Sun, J., and Fang, Y.: Effects of climate change on annual streamflow using climate elasticity in Poyang Lake Basin, China, Theor. Appl. Climatol., 112, 169–183, 2013.

Sun, Y., Tian, F., Yang, L., and Hu, H.: Exploring the spatial variability of contributions from climate variation and change in catchment properties to streamflow decrease in a mesoscale basin by three different methods, J. Hydrol., 508, 170–180, 2014.

Tang, B., Tong, L., Kang, S., and Zhang, L.: Impacts of climate variability on reference evapotranspiration over 58 years in the Haihe River Basin of north China, Agr. Water Manage., 98, 1960–1970, 2011.

Tang, Q., Oki, T., Kanae, S., and Hu, H.: The influence of precipitation variability and partial irrigation within grid cells on a hydrological simulation, J. Hydrometeorol., 8, 499, 2007.

Tang, Y., Tang, Q., Tian, F., Zhang, Z., and Liu, G.: Responses of natural runoff to recent climatic variations in the Yellow River basin, China, Hydrol. Earth Syst. Sci., 17, 4471–4480, doi:10.5194/hess-17-4471-2013, 2013.

Vogel, R. M., Wilson, I., and Daly, C.: Regional regression models of annual streamflow for the United States, J. Irrig. Drain. E.-ASCE, 125, 148–157, 1999.

Wang, Z., Shen, Y., and Song, L.: Hydrologic response of the climatic change based on SWAT Model in Beijiang River Basin, Meteorol. Environ. Res., 01, 8–12, 2013.

Water Resources and Hydropower Planning and Design General Institute: Specification for Comprehensive Water Resources Zoning, China Water & Power Press, Beijing China, 2011.

Xu, X., Yang, H., Yang, D., and Ma, H.: Assessing the impacts of climate variability and human activities on annual runoff in the Luan River Basin, China, Hydrol. Res., 44, 940–952, 2013.

Yang, D., Herath, S., and Musiake, K.: Development of geomorphology-based hydrological model for large catchments, Proc. Hydraul. Eng., 42, 169–174, 1998.

Dominant climatic factor driving annual runoff change at catchments scale over China

Z. Huang and H. Yang

⏮ | ⏭

◀ | ▶

Back | Close

Full Screen / Esc

Printer-friendly Version

Interactive Discussion

Yang, D., Herath, S., and Musiake, K.: Comparison of different distributed hydrological models for characterization of catchment spatial variability, Hydrol. Process., 14, 403–416, 2000.

Yang, D., Li, C., Hu, H., Lei, Z., Yang, S., Kusuda, T., Koike, T., and Musiake, K.: Analysis of water resources variability in the Yellow River of China during the last half century using historical data, Water Resour. Res., 40, 308–322, 2004.

Yang, D., Sun, F., Liu, Z., Cong, Z., and Lei, Z.: Interpreting the complementary relationship in non-humid environments based on the Budyko and Penman hypotheses, Geophys. Res. Lett., 33, 122–140, 2006.

Yang, H. and Yang, D.: Derivation of climate elasticity of runoff to assess the effects of climate change on annual runoff, Water Resour. Res., 47, 197–203, 2011.

Yang, H., Yang, D., Lei, Z., and Sun, F.: New analytical derivation of the mean annual water–energy balance equation, Water Resour. Res., 44, 893–897, 2008.

Yang, H., Qi, J., Xu, X., Yang, D., and Lv, H.: The regional variation in climate elasticity and climate contribution to runoff across China, J. Hydrol., 517, 607–616, 2014.

Zheng, H., Zhang, L., Zhu, R., Liu, C., Sato, Y., and Fukushima, Y.: Responses of streamflow to climate and land surface change in the headwaters of the Yellow River Basin, Water Resour. Res., 45, 641–648, doi:10.1029/2007WR006665, 2009.

Table 1. Principal parameters of Penman equation.

Symbol	Unit	Value	Physical meaning
Δ	$kPa\,°C^{-1}$	–	slope of the saturated vapor pressure vs. air temperature curve
R_n	$MJ\,m^{-2}\,d^{-1}$	–	net radiation
G	$MJ\,m^{-2}\,d^{-1}$	–	soil heat flux
γ	$kPa\,°C^{-1}$	–	psychrometric constant
λ	$MJ\,kg^{-1}$	2.45	latent heat of vaporization
e_s	kPa	–	saturated vapor pressure
RH	%	–	relative humidity
U_2	$m\,s^{-1}$	–	wind speed at a height of 2 m

Table 2. Principal parameters of Eq. (12).

Symbol	Unit	Value	Physical meaning
α_s	dimensionless	–	albedo or the canopy reflection coefficient
R_s	$MJ\,m^{-2}\,day^{-1}$	–	solar radiation
σ	$MJ\,K^{-4}\,m^{-2}\,day^{-1}$	4.903×10^{-9}	Stefan–Boltzmann constant
T_{max}	˚C	–	daily maximum air temperature
T_{min}	˚C	–	daily minimum air temperature
n	h	–	daily actual sunshine duration
N	h	–	daily maximum possible duration of sunshine
RH	%	–	daily relative humidity

Table 3. Comparison between the climate contribution to runoff by using the climate elasticity method and by using the hydrological models.

Catchments	Upper Hanjiang River Basin	Lower Luan River Basin	Upper Hanjiang River Basin
$\overline{P}$	402.4	512.4	850.0
$\overline{E_0}$	1257.4	1207.5	1178.0
$\Delta P/\overline{P}$	−9.8 %	1.8 %	−11.3 %
$\Delta E_0/\overline{E_0}$	−6.2 %	−8.0 %	3.0 %
ΔR	34.0	92.6	352.0
$(\Delta R/R)_O$	−30.8 %	−31.4 %	−27.6 %
n	1.4	1.4	1.0
ε_P	2.2	2.1	1.6
ε_{E_0}	−1.2	−1.1	−0.6
$(\Delta R/R)_M$	−14.0 %	12.4 %	−19.6 %
$(\Delta R/R)_E$	−21.4 %	9.1 %	−19.0 %

$\overline{P}$ is the mean annual precipitation (mm); $\overline{E_0}$ is mean annual potential evaporation (mm); $\Delta P/\overline{P}$ is the percentage of precipitation change (%);$\Delta E_0/\overline{E_0}$ is the percentage of potential evaporation change; ΔR is the runoff change (mm); $(\Delta R/\overline{R})_O$ is the percentage of runoff change that was observed; n is the characteristics parameter; ε_P and ε_{E_0} are the precipitation elasticity and potential evaporation elasticity, respectively; $(\Delta R/R)_M$ and $(\Delta R/R)_E$ are the percentage of runoff change that was estimated by hydrological models and the climate elasticity method, respectively.

Title Page

Abstract | Introduction

Conclusions | References

Tables | Figures

◄ | ►

◄ | ►

Back | Close

Full Screen / Esc

Printer-friendly Version

Interactive Discussion
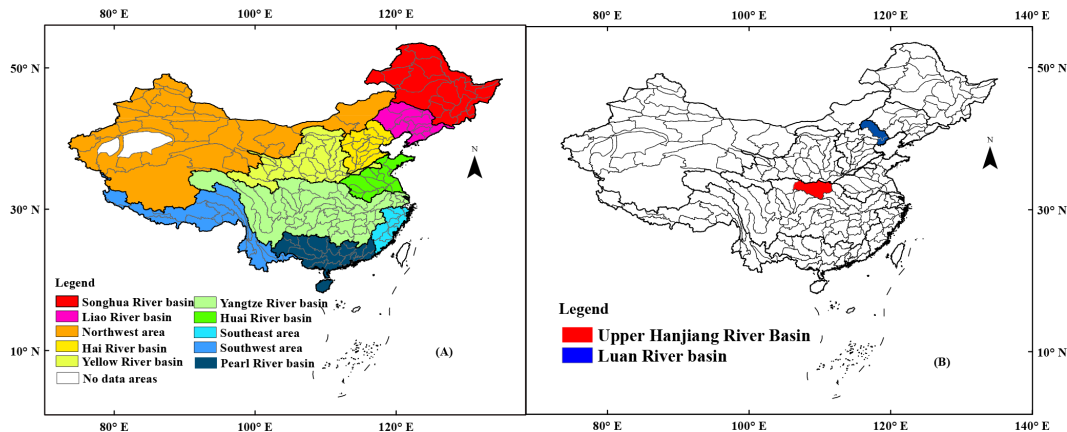
Figure 1. (a) Spatial distribution of the third-level river basins in China and **(b)** two basins for validation.
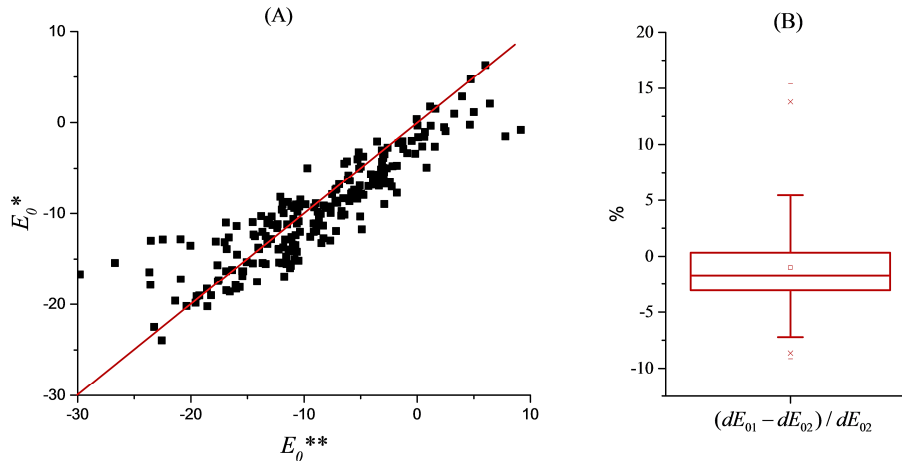
Figure 2. (a) Comparison between the potential evaporation change evaluated by equation Eq. (9), denoted as E_0^* (%) and that evaluated by Eq. (17) denoted as E_0^{**} (%) from 1961–2010, and **(b)** the relative error (%) caused by the first-order approximation, where dE_{01} and dE_{02} are the potential evaporation change (mm) calculated by Eq. (9) and that by Eq. (17), respectively.
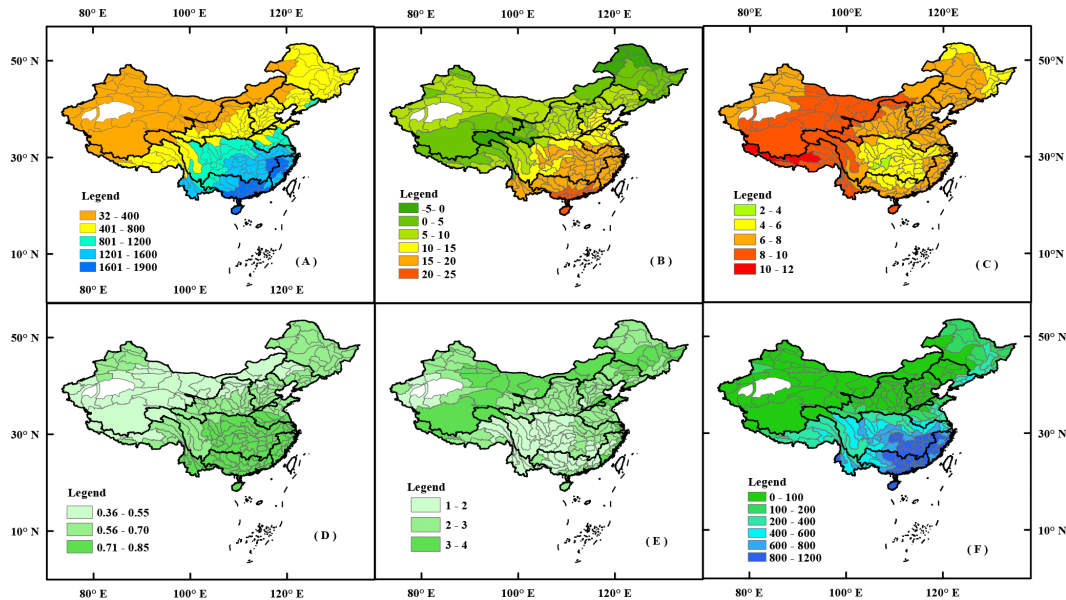
Figure 3. The mean annual **(a)** precipitation (unit: mm), **(b)** air temperature (unit: °C), **(c)** net radiation (unit: $MJ\,m^{-2}\,day^{-1}$), wind speed, **(d)** relative humidity, **(e)** wind speed in 2 m height (unit: $m\,s^{-1}$), and **(f)** runoff (unit: mm) in the 207 catchments during 1961–2010.
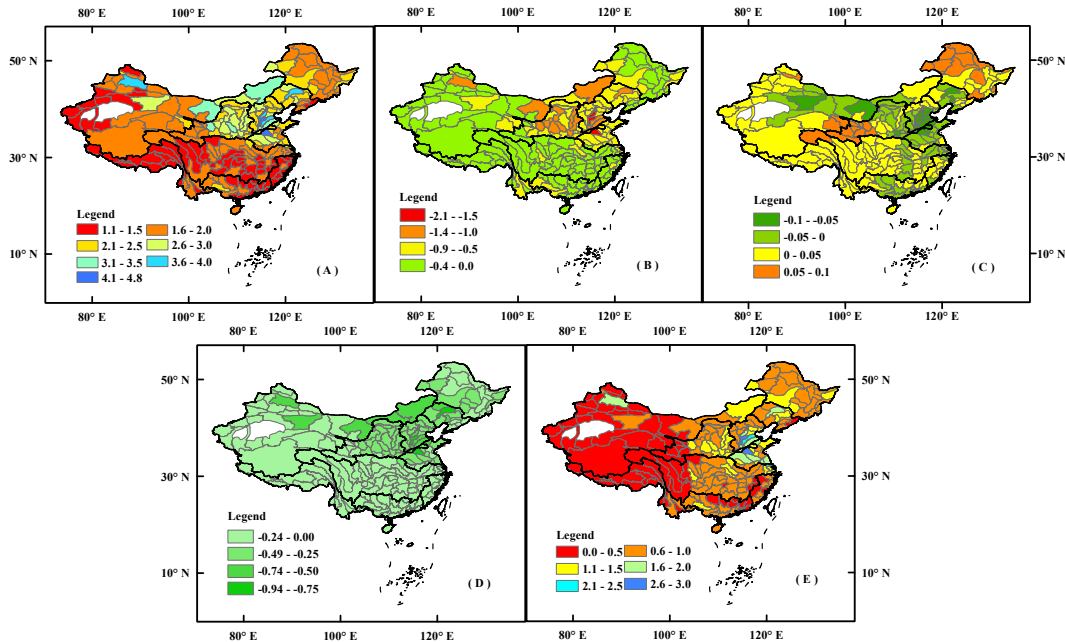
Figure 4. (a) Precipitation elasticity ε_P, **(b)** net radiation elasticity ε_{R_n}, **(c)** air temperature elasticity ε_T, **(d)** wind speed elasticity ε_{U_2} and **(e)** relative humidity elasticity ε_{RH} of runoff in the 207 catchments.
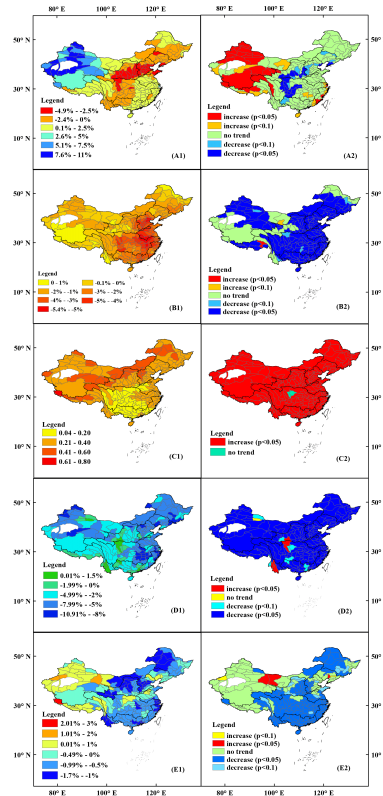
Figure 5. The changing trends for **(a1)** precipitation (unit: decade^{-1}), **(b1)** net radiation (unit: decade^{-1}), **(c1)** air temperature (unit: decade^{-1}), **(d1)** wind speed (unit: decade^{-1}), **(e1)** relative humidity (unit: decade^{-1}); and the significance of the trends for **(a2)** precipitation, **(b2)** net radiation, **(c2)** air temperature, **(d2)** wind speed, **(e2)** relative humidity to runoff in the 207 catchments from 1961–2010.
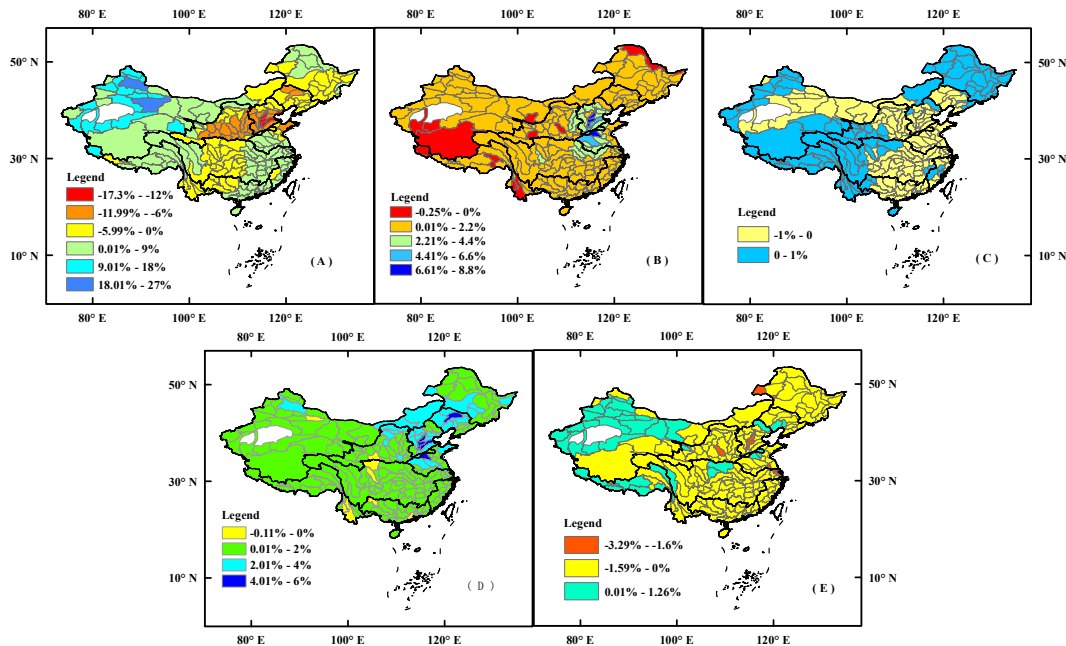
Figure 6. The contribution of **(a)** precipitation, **(b)** net radiation, **(c)** air temperature, **(d)** wind speed, **(e)** relative humidity to runoff in the 207 catchments from 1961–2010 (unit: decade^{-1}).
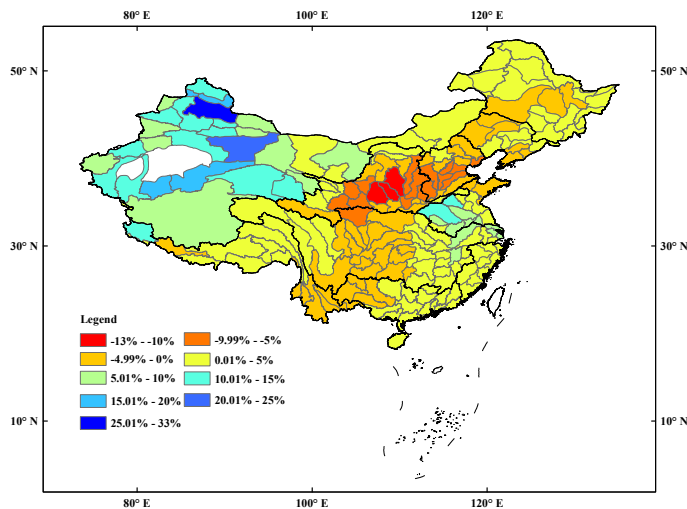
Figure 7. The effect of climate change to runoff in the 207 catchments from 1961 to 2010 (unit: decade^{-1}).
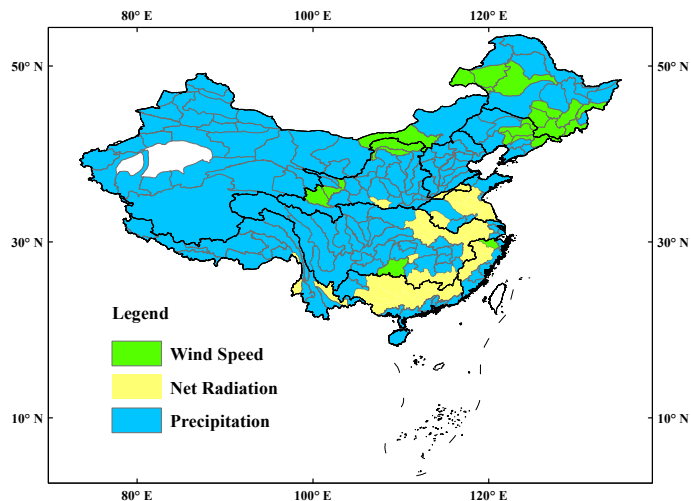
**Figure 8.** Dominant climatic factor driving annual runoff change in the 207 catchments from 1961 to 2010.

Figure 9. Relationship between T and $\frac{\partial E_0}{\partial T}$ in the 207 basins of China.
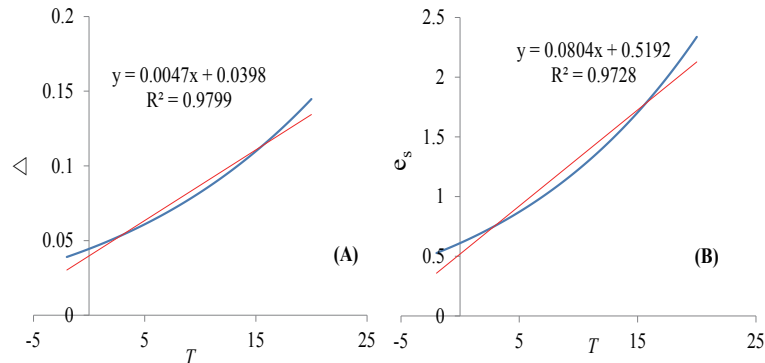
Figure 10. Relationship of **(a)** Δ and **(b)** e_s with temperature change. The blue curves are the relationship Δ of and e_s with T, respectively; the pink curves show the linear slope of Δ and e_s with T (T ranging from -2 to $20\,°C$), respectively.

In figure (A): $y = 0.0047x + 0.0398$, $R^2 = 0.9799$

In figure (B): $y = 0.0804x + 0.5192$, $R^2 = 0.9728$